

RESEARCH ARTICLE

Phosphotransferase system sugars immediately induce mutations of *Cra* in an *Escherichia coli ptsH* mutant

Huitae Min | Yeong-Jae Seok

School of Biological Sciences and Institute of Microbiology, Seoul National University, Seoul, Republic of Korea

Correspondence

Yeong-Jae Seok, School of Biological Sciences and Institute of Microbiology, Seoul National University, Seoul 08826, Republic of Korea.
Email: yjseok@snu.ac.kr

Funding information

Ministry of Science, South Korea, Grant/Award Numbers: NRF-2018R1A5A1025077, NRF-2019R1A2C2004143; National Research Foundation

Abstract

Most bacteria use the phosphoenolpyruvate (PEP):sugar phosphotransferase system (PTS) to catalyse coupled transport and phosphorylation of sugars. The PTS consists of several sugar-specific components (enzyme IIs) and two general components: enzyme I, encoded by *ptsI*, and HPr, encoded by *ptsH*, which are common to most PTS carbohydrates. Although both enzyme I and HPr are believed to be required to utilize these PTS sugars, an *E. coli ptsH* mutant has been reported to exhibit a leaky growth phenotype on these sugars. Here, we show that this phenomenon occurs because the *ptsH* mutant undergoes adaptive mutations in the presence of PTS sugars within a few generation times. The *ptsH* mutant cells once exposed to a PTS sugar showed a growth rate similar to that of the wild-type strain when transferred to fresh medium supplemented with the same PTS sugar, suggesting the acquisition of additional genetic variations. Genome sequencing revealed that the PTS sugar-adapted variants harboured loss-of-function mutations in *cra*, which increased expression of the *fruBKA* operon. Our results suggest that the presence of a PTS sugar can exert a strong selective pressure when a general PTS component is defective.

INTRODUCTION

Most organisms utilize carbohydrates as carbon and energy sources, with most bacteria using the phosphoenolpyruvate (PEP):sugar phosphotransferase system (PTS) to transport carbohydrates, such as glucose (Figure S1A) (Deutscher et al., 2006, 2014). The PTS consists of two general components, namely, enzyme I (EI) and HPr, required to utilize most PTS sugars and several sugar-specific components known as enzyme IIs (EIIs). Each EII consists of two cytoplasmic domains (EIIA and EIIB) and one or two membrane domains (EIIC or EIID). EI catalyses the phosphoryl transferase reaction from the glycolytic intermediate PEP to HPr. Subsequently, HPr transfers the phosphoryl group to the various EIIs and then to EIIBs. Finally, PTS sugars are transported across the membrane through EIICs (and EIIDs) and simultaneously phosphorylated by EIIBs.

PTS components can substantially change in their phosphorylation status depending on the exogenous sugar source (Hogema et al., 1998). The ratio of

phosphorylated and dephosphorylated PTS components provides signals for regulating various physiological processes and metabolic pathways (Deutscher et al., 2006; Gorke & Stulke, 2008). For example in *E. coli*, during glucose consumption, EIIA^{Glc} (a glucose-specific EIIA component) is dephosphorylated and blocks several non-PTS permeases such as lactose permease, by direct interaction (Postma et al., 1993). In contrast, phosphorylated EIIA^{Glc} has a distinct physiological role in facilitating the transport and metabolism of non-PTS sugars by activating adenyl cyclase, which converts ATP to cyclic AMP (cAMP) (Park et al., 2006). Dephosphorylated HPr, accumulated during glucose transport, interacts with the mannitol operon regulator, MtlR, and enhances its repressor activity (Choe et al., 2017). Dephosphorylated HPr also binds to Rsd and antagonizes both its anti- σ^{70} activity and stimulatory effect on SpoT (p)ppGpp hydrolase activity (Lee et al., 2018; Park et al., 2013).

Unlike other PTS sugars, fructose is transported through a unique transport mechanism in various

bacterial families and species (Comas et al., 2008). In the families *Enterobacteriaceae* (e.g. *Escherichia coli*) and *Vibrionaceae* (e.g. *Vibrio cholerae*), FruB, a fructose PTS component, consists of three domains: EIIA, M (central domain), and FPr (fructose-inducible HPr-like domain). For fructose utilization, FruB, rather than HPr and EIIA, catalyses the phosphotransferase reaction between EI and the EIIB domain (Figure S1B). Notably, transposon mutagenesis studies have suggested that the overexpression of FruB in *E. coli* and *Salmonella typhimurium* can replace the phosphotransferase activity of HPr in PTS sugar transport (Geerse et al., 1986; Monedero et al., 1998).

Various adaptive laboratory evolution models have reported that microorganisms, including *E. coli*, can undergo adaptive genomic mutations to survive under several extreme laboratory conditions such as oxygen restriction, phage infection, and nutrient transporter deficiency (Poursat et al., 2019; Shewaramani et al., 2017; Taylor, 1963; Warsi et al., 2018). Since the PTS is involved in regulating various physiological mechanisms, such as metabolic gene expression and the activity of several sugar permeases, the inactivation of a general PTS component in *E. coli* results in growth defects on various carbon sources, including both PTS and non-PTS sugars (Postma et al., 1993). Nevertheless, a *ptsH* mutant has been shown to exhibit a leaky growth phenotype on some sugars (Baba et al., 2006; Simoni et al., 1976). This study investigates how rapidly the *ptsH* mutant of *E. coli* undergoes spontaneous adaptive mutations in the presence of various sugars, thereby assessing the ability of bacteria to actively cope with stressful environments for survival. This adaptive molecular mechanism may shed light on the evolutionary vestiges of the PTS.

EXPERIMENTAL PROCEDURES

Bacterial strains, plasmids, and culture conditions

The *Escherichia coli* strains and plasmids used in this study are listed in Table S2. *Escherichia coli* cells were grown at 37 °C in LB medium or M9 minimal medium containing the indicated amount of sugars in culture flasks or 96-well plates with shaking at 200 rpm. All plasmids in this study were constructed using standard PCR-based cloning procedures and verified by sequencing. In-frame deletion mutants in this study were constructed using the pKD46 plasmid, as previously described (Datsenko & Wanner, 2000).

Genomic DNA extraction and sequencing

Stocks of *E. coli* strains were inoculated into 15 ml of LB medium in a 50 ml conical tube and incubated at

37°C on a 200 rpm orbital shaker. After cells were harvested, and their genomic DNA (gDNA) was isolated using a QIAamp DNA Mini Kit (Qiagen). The contamination of the extracted gDNA by other genomes was ruled out using amplification and sequencing of the 16 S rRNA gene. The purity and concentration of the extracted gDNA were determined using a Qubit 2.0 fluorometer (Invitrogen).

Whole-genome sequencing and assembly were performed at Macrogen Inc. (Seoul, Korea) using an Illumina HiSeq 2500 platform. To generate libraries, 400 ng of gDNA was fragmented into 550 bp using a M220 Focused-ultrasonicator™ (Covaris), and the fragmented DNA was quantified using a DNA 7500 kit (Agilent) and a Bioanalyzer 2100 instrument (Agilent). The library was constructed using the TruSeq DNA Library LT kit (Illumina) following the manufacturer's protocols. Whole-genome analysis was performed on the Illumina HiSeq 2500 system with 2 × 300 bp paired-end reads. The obtained sequencing data were assembled with SPAdes 3.9.1 and annotated by homology searches using USEARCH v8.1.1861 against *E. coli* K-12 substr. MG1655 gDNA sequence.

RNA extraction and quantitative real-time reverse transcription-PCR

RNA extraction and quantitative real-time reverse transcription-PCR (qRT-PCR) were performed as previously described (Choe et al., 2017). Cells were cultivated at 37°C in LB medium or M9 medium supplemented with the indicated amount of sugars and harvested in the early exponential phase. Total RNA was then isolated using an RNeasy Mini Kit (Qiagen), and gDNA was removed using RNase-free DNase I (Promega). cDNA was synthesized from the total RNA (2500 ng) using the cDNA EcoDry™ Premix (Clontech Laboratories, Inc.). The 30-fold diluted cDNA was subjected to qRT-PCR analyses using gene-specific primers and a FAST SYBR™ green master mix kit (Life Technologies). The CFX96 Real-Time System (Bio-Rad) was used to amplify and detect the qRT-PCR product. The transcript level of *rrsH* was used for data normalization.

Purification of proteins

Proteins with N-terminal His tags used in this study were overproduced in *E. coli* ER2566 (New England Biolabs)/pETDuet-1 (Novagen) by adding 1 mM isopropyl β-D-thiogalactoside. Harvested cells containing overexpressed proteins were resuspended in binding buffer (20 mM Tris-HCl [pH 7.5], 100 mM NaCl, 0.05% β-mercaptoethanol, 10% glycerol) and disrupted by three passages through a French pressure cell at

9000 psi. After centrifugation at $9300 \times g$ and 4°C for 30 min, the supernatant was loaded onto a Poly Prep chromatography column (8×40 mm; Bio-Rad) with TALON metal-affinity resin (Takara Bio). The column was washed three times with wash buffer (10 mM imidazole added to binding buffer) and the bound proteins were eluted with elution buffer (200 mM imidazole added to binding buffer). To remove imidazole and increase the purity of proteins, the pool was chromatographed on a HiLoad 16/60 Superdex 75 prep grade column (GE Healthcare Life Sciences) equilibrated with a binding buffer. The purified proteins were stored at -80°C until use.

Electrophoretic mobility shift assay

Electrophoretic mobility shift assay (EMSA) was performed without using radioactivity as previously described (Yoon et al., 2021). A 150-bp *fruB* probe containing two Cra-binding sites was amplified by PCR using the *E. coli* MG1655 chromosome as a template. The probe was mixed with Cra or its variant in TGED buffer (10 mM Tris-HCl [pH 8.0], 5% glycerol, 0.1 mM EDTA, and 1 mM DTT), and $200 \mu\text{g ml}^{-1}$ bovine serum albumin as non-specific protein competitor. Each sample was incubated at 37°C for 15 min and loaded on a 6% polyacrylamide gel (acrylamide/bisacrylamide ratio of 29:1) in TBE (89 mM Tris, 89 mM boric acid, and 20 mM EDTA) followed by staining with Green Star nucleic acid staining solution (Bioneer). DNA bands were visualized using DUALED Blue/White Transilluminator (Bioneer).

Determination of the in vivo phosphorylation state of EIIA^{Glc}

The phosphorylation state of EIIA^{Glc} was determined as previously described with some modifications (Takahashi et al., 1998; Lee et al., 2019). Since phosphohistidine residues are very unstable at neutral and acidic pH, exposure of samples to pH <8.0 was minimized. *E. coli* strains were cultivated in LB or M9 minimal medium containing glucose or lactose. Cell cultures (0.2 ml at OD₆₀₀ of 0.2) were quenched, the phosphorylation states of EIIA^{Glc} were fixed, and the cells were disrupted at the same time by mixing with $20 \mu\text{l}$ of 5 M NaOH, followed by vortexing for 20 s. After the addition of $80 \mu\text{l}$ of 3 M sodium acetate (pH 5.2) and 0.7 ml of ethanol, the samples were centrifuged at $10,000 \times g$ at 4°C for 15 min. The pellets were then suspended in $40 \mu\text{l}$ of SDS sample buffer (2% SDS, 5% 2-mercaptoethanol, 62.5 mM Tris-HCl [pH 8.0], 10% glycerol, 0.1% bromophenol blue), and $30 \mu\text{l}$ of each sample was immediately analysed using 16% SDS-polyacrylamide gel electrophoresis. Western blotting was performed as previously described (Park et al., 2013).

Determination of the intracellular cAMP level

The intracellular cAMP level was determined as previously described with some modifications (Park et al., 2006). *E. coli* strains were cultivated in M9 minimal medium containing lactose, maltose, or glycerol. The pellet was suspended in a reaction volume of $50 \mu\text{l}$ Bicine buffer (25 mM bicine [pH 8.5], 10 mM MgCl₂, 1 mM ATP, 2 mM dithiothreitol, 20 mM Na₂HPO₄, 200 mM NaCl) and incubated at room temperature for 10 min. The samples were withdrawn into $50 \mu\text{l}$ of 1 M perchloric acid and then centrifuged at $10,000 \times g$ at 4°C for 10 min. Their supernatants were analysed to determine cAMP concentration using the cAMP enzyme immunoassay kit (Amersham Biosciences).

RESULTS

PTS sugar exerts strong selective pressure on the *ptsH* mutant for immediate adaptive mutations

A previous study showed that incubation of the *E. coli* PB11 strain lacking both EI and HPr in an M9-glucose medium for longer than 70 h induced a loss-of-function in *galR*, leading to overexpression of a galactose:H⁺-symporter GalP (Aguilar et al., 2012). GalP was previously shown to have a weak glucose permease activity (Hernandez-Montalvo et al., 2003). In addition, it was reported that several *S. typhimurium* strains, lacking both EI and HPr, can regain the ability to specifically utilize glucose by the constitutive synthesis of a galactose permease (Saier et al., 1973). Although it is well known that both EI and HPr are indispensable for the growth on various sugars (Postma et al., 1993), the *ptsH* mutants, unlike *ptsI* mutants, of *E. coli* and *S. typhimurium* have been shown to exhibit leaky growth phenotypes on various sugars (Baba et al., 2006; Simoni et al., 1976). This led us to investigate whether and how the two mutants exhibit different growth phenotypes on PTS and non-PTS sugars (Figures 1 and S2, respectively). Our growth tests showed that the *ptsH* mutant exhibited retarded growth on various sugars as the sole carbon source but reached exponential growth within 2 days, whereas the *ptsI* mutant did not grow. When the *ptsH* mutant cells grown twice on a non-PTS sugar (lactose, maltose, or glycerol) were transferred to the fresh medium containing the same non-PTS sugar, the growth retardation was still observed (Figure S2). However, when the *ptsH* mutant cells grown once on a PTS sugar (glucose, mannitol, mannose, or *N*-acetylglucosamine [NAG]) were transferred to the fresh medium containing the same PTS sugar, they showed similar growth patterns to the wild-type cells and no growth retardation was

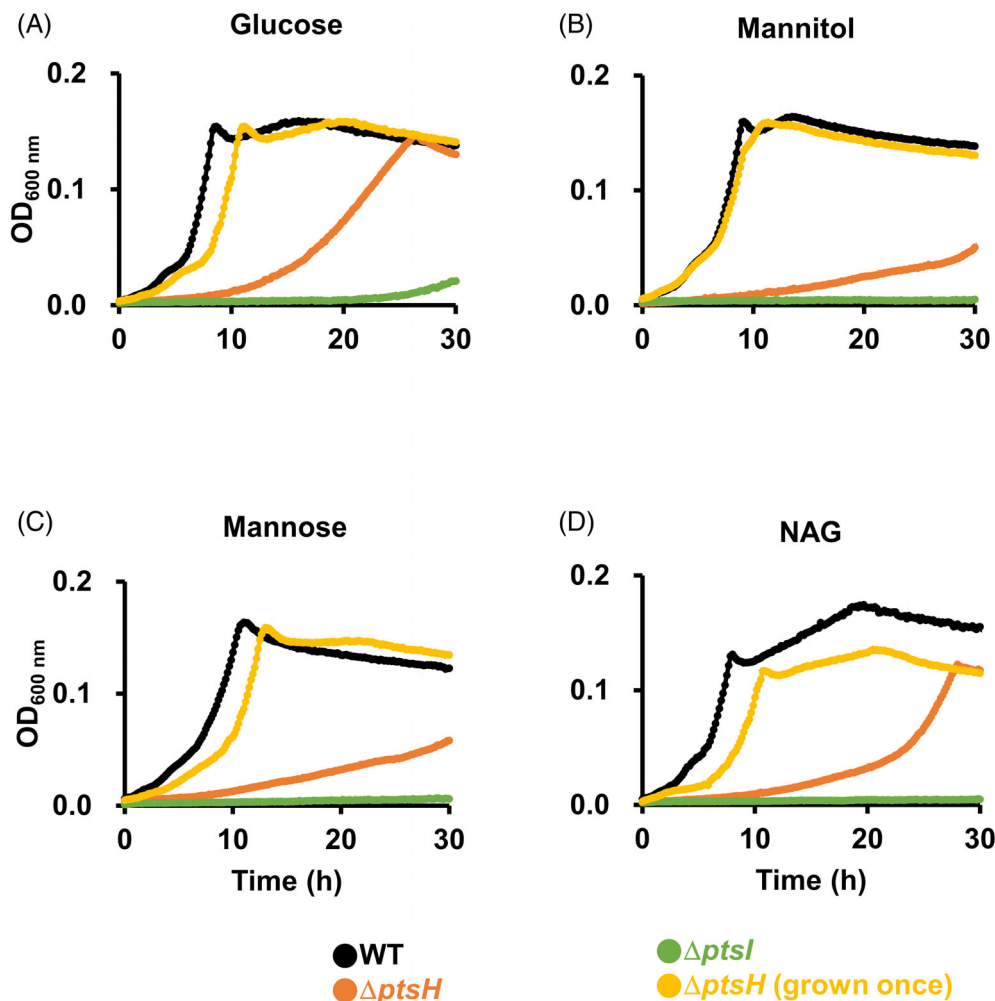


FIGURE 1 The *ptsH* mutant undergoes genetic changes in the presence of PTS sugars. The *ptsH* deletion mutant and *ptsI* deletion mutant of the *E. coli* K12 strain MG1655 were incubated in an M9 minimal medium supplemented with 0.04% glucose (A), mannitol (B), mannose (C), or *N*-acetylglucosamine (NAG) (D), and their growth was compared to that of the wild type in a 96-well plate by recording the absorbance at 600 nm using a multimode microplate reader (TECAN). The *ptsH* mutant cells grown once on each sugar were incubated and their growth was recorded under identical conditions. Data shown are the averages of three measurements.

observed (Figure 1). Accordingly, we assumed that PTS sugars might have induced adaptive genetic mutations in the *ptsH* mutant even in the absence of a mutagen. To verify this assumption, single colonies of wild-type and the *ptsH* mutant strain were picked from LB plates and grown overnight in LB broth. Approximately 100 colony-forming units (CFUs) of the wild type or 100,000 CFUs of the *ptsH* mutant were then plated on an M9 agar medium supplemented with a PTS or non-PTS sugar as the sole carbon source with and without preincubation in M9 medium containing the same sugar for 1 h (Figure 2). When incubated at 37 °C for 30 h, the wild-type strain formed similar numbers of colonies regardless of preincubation and carbon source, indicating that the first cell division did not take place within 1 h after the LB-to-M9 transition regardless of the carbon source. Interestingly, however, while the *ptsH* mutant formed no conspicuous colonies on M9 agar plates containing non-PTS sugars within 30 h

regardless of preincubation, the preincubation with a PTS sugar for 1 h increased CFUs of the *ptsH* mutant more than 10-fold on an M9 agar plate containing the same PTS sugar (Figure 2B). Based on these results, we assumed that PTS sugars increase mutation rates of the *ptsH* mutant to approximately 6×10^{-4} per cell per hour. Therefore, it is reasonable to conclude that PTS sugars, but not non-PTS sugars, can induce immediate adaptive genetic changes in the *ptsH* mutant, resulting in its leaky growth phenotypes on a PTS sugar.

Leaky growth phenotype of the *ptsH* mutant on PTS sugars is due to immediate loss-of-function mutations in *cra*

To elucidate the mechanism of genetic mutations induced by PTS sugars in the *ptsH* mutant, we

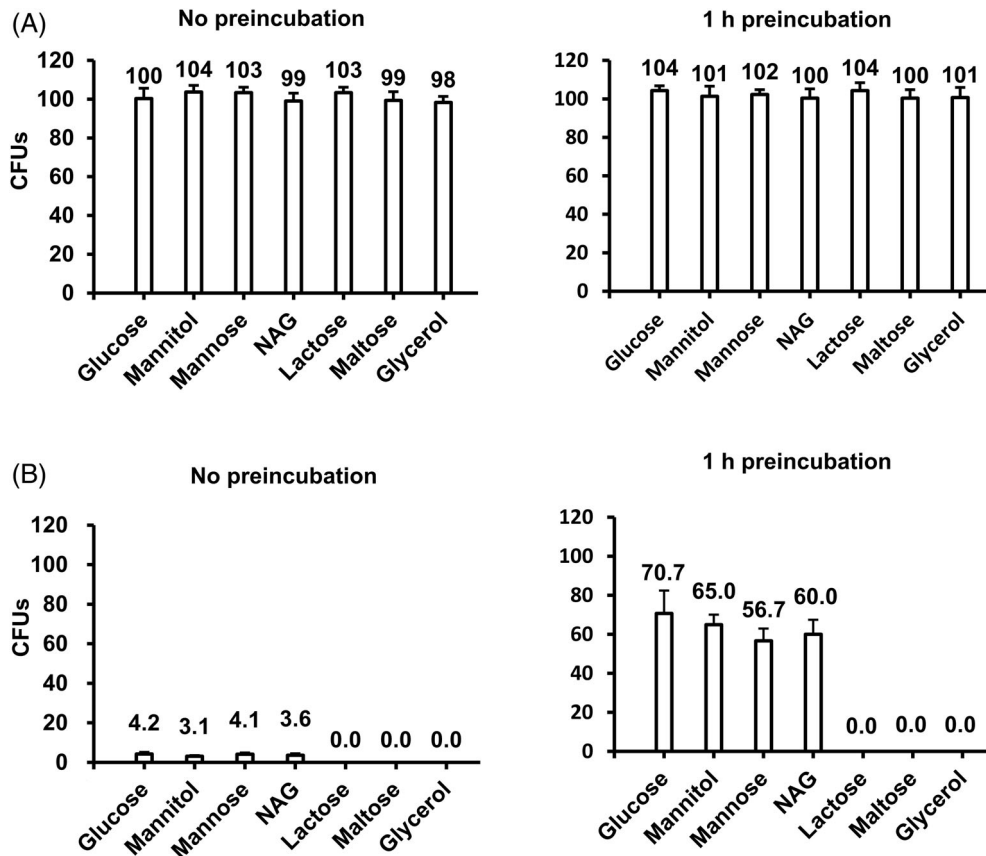


FIGURE 2 PTS sugars exert strong selective pressure on the *ptsH* mutant for immediate adaptive mutations. Single colonies of wild-type (A) and the *ptsH* mutant (B) of the *E. coli* K12 strain MG1655 were picked from an LB plate and grown overnight in LB broth. Approximately 100 CFUs of the wild type or 100,000 CFUs of the *ptsH* mutant were then plated on an M9 agar medium supplemented with 0.2% of the indicated carbon source with or without preincubation in M9 medium containing the same sugar for 1 h. After incubating at 37 °C for 30 h, the number of colonies was counted. Data shown (means \pm SD) are from three independent experiments.

performed a whole-genome sequence analysis of the largest colony of the *ptsH* mutant cells adapted to rapid growth on glucose (*ptsH* GA1 strain) in comparison to the parental *ptsH* mutant and the wild-type K-12 strain MG1655. Two point mutations were detected in the genomic DNA of *ptsH* GA1, one (Tyr 19 to Cys, Y19C) in the DNA-binding domain of Cra, a repressor of the *fruBKA* operon, and the other (V11D) in the signal sequence of OmpF, a general outer membrane porin. Therefore, we sequenced *cra* and *ompF* genes from all visible *ptsH* mutant colonies (*ptsH* PA) from Figure 2B (left panel). As a result, while no mutations in *ompF* were detected in other *ptsH* PA strains, all of them without exception carried various types of mutations in *cra*, suggesting that the adaptation of the *ptsH* mutant to PTS sugar might be due to an additional mutation in *cra* (Table S1). Most additional mutations caused premature chain termination (PCT) due to nonsense or frameshift mutation, resulting in loss of Cra function. Exceptionally, we identified two missense mutations in the DNA-binding domain of Cra (Y19C and L3M).

According to previous transposon mutagenesis studies, FruB overexpression, induced by loss of Cra

function, could replace the phosphotransferase activity of HPr in PEP-dependent transport and phosphorylation of PTS sugars (Geerse et al., 1986; Monedero et al., 1998). GalR-LacI family transcription factors, including *E. coli* Cra, bind to tandem binding sites and induce DNA looping as tetramers (Negre et al., 1996; Ramseier, 1996). A previous study identified many DNA-binding sites for Cra in the *E. coli* genome, including two binding sites in the *fruB* promoter region (Shimada et al., 2005). To verify whether the two Cra variants (Y19C and L3M) lost DNA-binding affinity, we performed an electrophoretic mobility shift assay (EMSA) with a 150-bp DNA probe containing the two binding sites in the *fruB* promoter region (Figure S3). When the probe was incubated with increasing amounts of wild-type Cra, there were two shifted bands produced by the formation of the DNA-protein complexes. However, the Cra variant (Y19C or L3M) showed lower DNA-binding affinity compared to the wild type. This result is consistent with a previous study that suggested Y19 (Tyr19) and L3 (Leu3) of Cra to be involved in its DNA contacts (Penin et al., 1997). Cra has been reported to not only repress the *fruBKA*

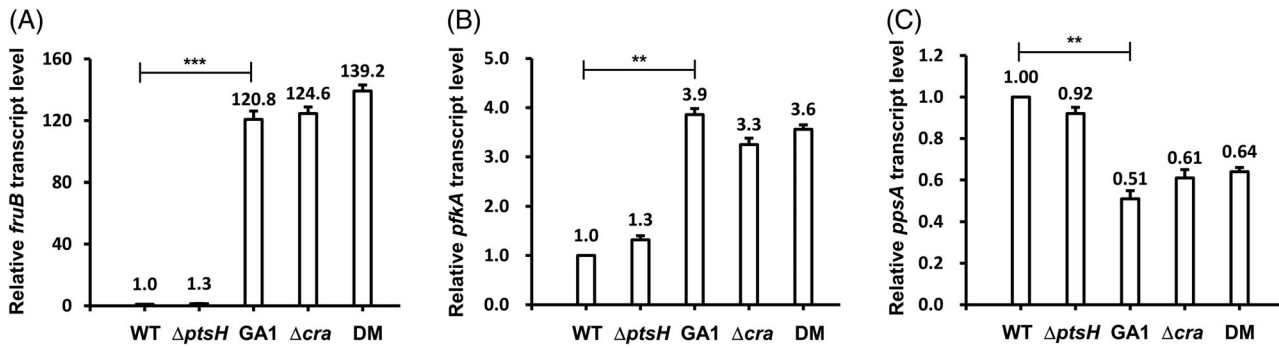


FIGURE 3 Loss of Cra function in *ptsH* GA1. Total RNA was extracted from the wild-type *E. coli* MG1655, *ptsH* mutant, *ptsH* GA1, *cra* mutant and *ptsH cra* double mutant (DM) grown to early exponential phase in LB medium, and the expression levels of *fruB* (A), *pfkA* (B), and *ppsA* (C) were quantified using qRT-PCR. Data shown (means \pm SD) are from three independent experiments. Statistical significance was determined via Student's *t*-test (** $p < 0.005$ and *** $p < 0.0005$).

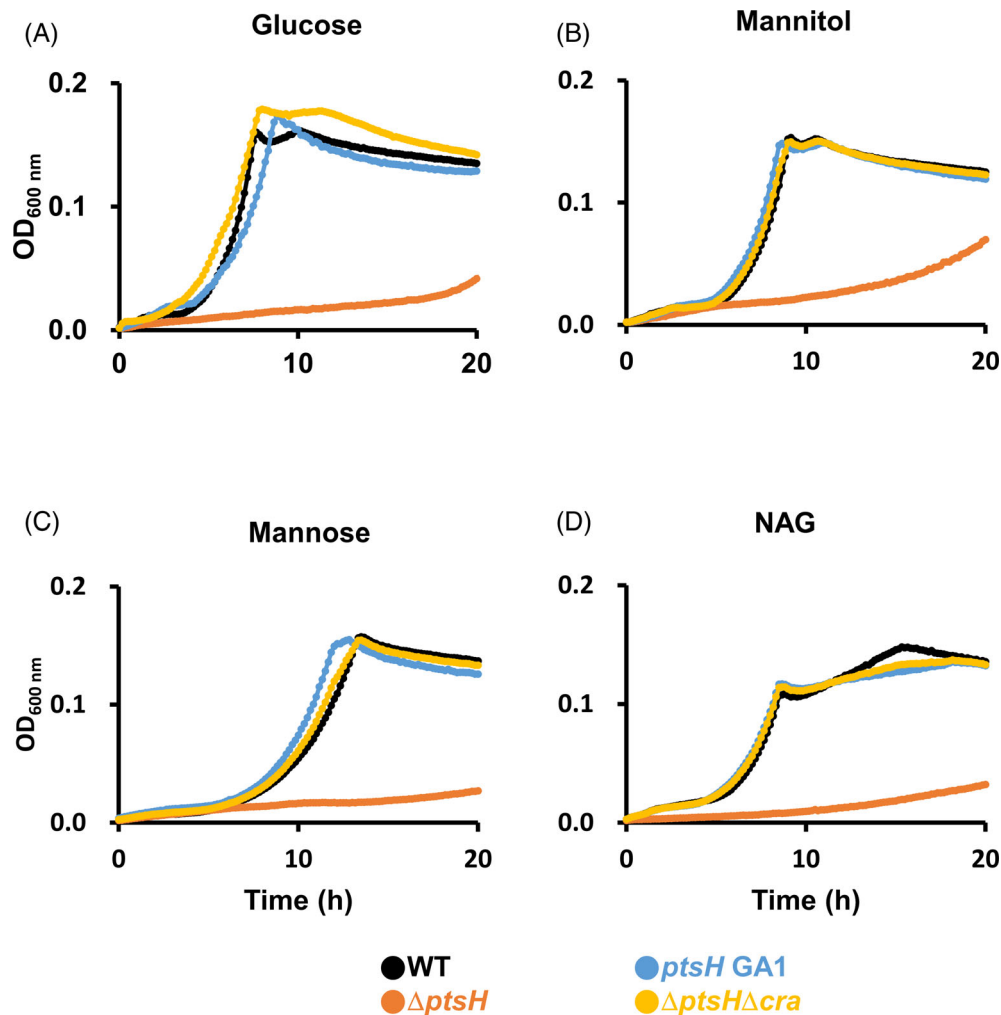


FIGURE 4 *ptsH* GA1 can utilize various PTS sugars. The *ptsH* GA1 strain was incubated in an M9 medium supplemented with 0.04% glucose (A), mannitol (B), mannose (C), or NAG (D) and its growth was compared to those of the wild type, *ptsH* mutant and *ptsH cra* double mutant in a 96-well plate by recording the absorbance at 600 nm using a multimode microplate reader (TECAN). Data shown are the averages of three measurements.

operon and several glycolytic genes, such as *pfkA* and *pykF*, but also activate the transcription of several gluconeogenesis-related genes, such as *fbp* and *ppsA*

(Kochanowski et al., 2013; Ramseier, 1996). To determine how the lowered binding affinity of the Cra variants affects the function of Cra in vivo, we examined

the transcriptional levels of *fruB*, *pfkA*, and *ppsA* in *ptsH* GA1 carrying the Y19C mutation (Figure 3). As expected, the expression level of *pfkA* was increased (~4-fold) and the expression level of *ppsA* was decreased (~2-fold) in *ptsH* GA1 compared to that of the wild-type strain. Moreover, the expression level of *fruB* in *ptsH* GA1 was significantly higher (~120-fold) than that in the wild-type strain and similar to that in the *cra* deletion mutant and *ptsH cra* double mutant. Therefore, we assumed that this increased level of FruB allowed *ptsH* GA1 to utilize other PTS sugars, such as mannitol, mannose, and NAG as efficiently as glucose (Figure 4). This assumption is supported by the observation that *ptsH* GA1 showed similar growth to that of the *ptsH cra* double mutant and a *ptsH* mutant strain adapted to rapid growth on mannitol (*ptsH* MA1 strain carrying a nonsense mutation in *cra*, see Table S1) could also utilize PTS sugars as efficiently as the wild-type strain (Figure S4). Therefore, we hypothesized that PTS sugars could exert a selective pressure and, consequently, cause immediate loss-of-function mutations in *cra* to increase FruB expression in the *ptsH* mutant.

To confirm that the leaky growth phenotype of the *ptsH* mutant on PTS sugars depends on immediate Cra mutations, we constructed the pBR322-derived expression vector for Cra (pCra) under the control of the *cat* promoter. We examined the growth of the *ptsH* mutant harbouring pCra during incubation with the PTS sugars as the sole carbon source (Figure S5). While the *ptsH* mutant showed slow but detectable growth on various PTS sugars (see also Figure 1), the *ptsH* mutant harbouring pCra did not show any apparent growth on these sugars within 30 h. In addition, the inactivation of *fruB* in the *ptsH* mutant or *ptsH* GA1 strain resulted in a complete loss of its growth on PTS sugars (Figure S6). Taken together, we concluded that the leaky growth phenotype of the *ptsH* mutant on PTS sugars is due to immediate loss-of-function mutations in *cra*.

The FPr domain of FruB can replace the phosphotransferase activity of HPr

In *E. coli*, FruB consists of three domains: EIIA, M, and FPr (Figure S1B) (Reizer et al., 1994). It is a diphosphoryl transfer protein, which contains two phosphorylatable histidine residues (H62 in the EIIA domain and H299 in the FPr domain). The FPr domain of FruB has ~37% amino acid sequence identity with HPr and the residues near H299 are more highly conserved than the other parts (Figure S7A,C) (Reizer et al., 1994). Therefore, given the increased expression of FruB (Figure 3A), we hypothesized that the FPr domain may replace the phosphotransferase activity of HPr in the PEP-dependent phosphorylation of PTS substrates. To

test this hypothesis, we constructed pBR322-derived expression vectors for two phosphorylation site mutants of FruB (pFruB-H62A and pFruB-H299A) and the wild-type FPr domain (pFPr) under the control of the *cat* promoter. We then compared the growth of the *ptsH* mutant harbouring pFruB-H62A, pFruB-H299A or pFPr with that of *ptsH* GA1 harbouring the control vector pBR322 on PTS sugars (Figure 5). While the pFruB-H299A could not rescue the growth defect of the *ptsH* mutant on PTS sugars, the *ptsH* mutant harbouring pFruB-H62A or pFPr showed similar growth to that of *ptsH* GA1 carrying the control vector pBR322 and the *ptsH* mutant harbouring wild-type FruB (pFruB). Taken together, we concluded that the FPr domain of FruB can replace the phosphotransferase activity of HPr in *ptsH* PA strains.

Cra mutations can restore growth of the *ptsH* mutant even on non-PTS sugars

Dephosphorylated EIIA^{Glc} binds and inactivates metabolic enzymes and transporters of non-PTS sugars, such as lactose permease, maltose ATP-binding cassette transporter, and glycerol kinase, by a mechanism known as inducer exclusion (Bluschke et al., 2006; Postma et al., 1993). In contrast, phosphorylated EIIA^{Glc} binds and activates adenylyl cyclase that converts ATP to cAMP, which is required for the transcription of several genes in the metabolism of non-PTS sugars (Park et al., 2006). Therefore, the parental *ptsH* mutant exhibited growth defects not only on PTS sugars but also on a range of non-PTS sugar such as lactose, maltose, or glycerol unless cAMP is added (Figures 1 and S2) (Postma et al., 1993), since EIIA^{Glc} cannot be phosphorylated in the absence of a general PTS component. Considering that *ptsH* PA strains could efficiently utilize various PTS sugars (Figure 5 and Figure S4), we assumed that EIIAs, including EIIA^{Glc}, could be phosphorylated by FruB in *ptsH* PA strains as efficiently as by HPr in the wild-type strain. As expected, EIIA^{Glc} was mostly dephosphorylated in M9 medium supplemented with glucose, whereas it was phosphorylated in M9 medium supplemented with lactose and LB medium in *ptsH* GA1 to levels comparable to the wild-type strain (Figure 6A). In agreement with this observation, *ptsH* GA1 and the *ptsH cra* double deletion mutant showed significantly faster growth on non-PTS sugars such as lactose, maltose, and glycerol than the parental *ptsH* mutant (Figure 6B-D). Taken together, we conclude that Cra mutations can restore growth of the *ptsH* mutant not only on PTS sugars but also on non-PTS sugars, as the increased expression of FruB can catalyse the phosphotransferase reaction between EI and EIIA^{Glc}, which might provide adequate intracellular levels of cAMP and overcome inducer exclusion. As expected, similar to

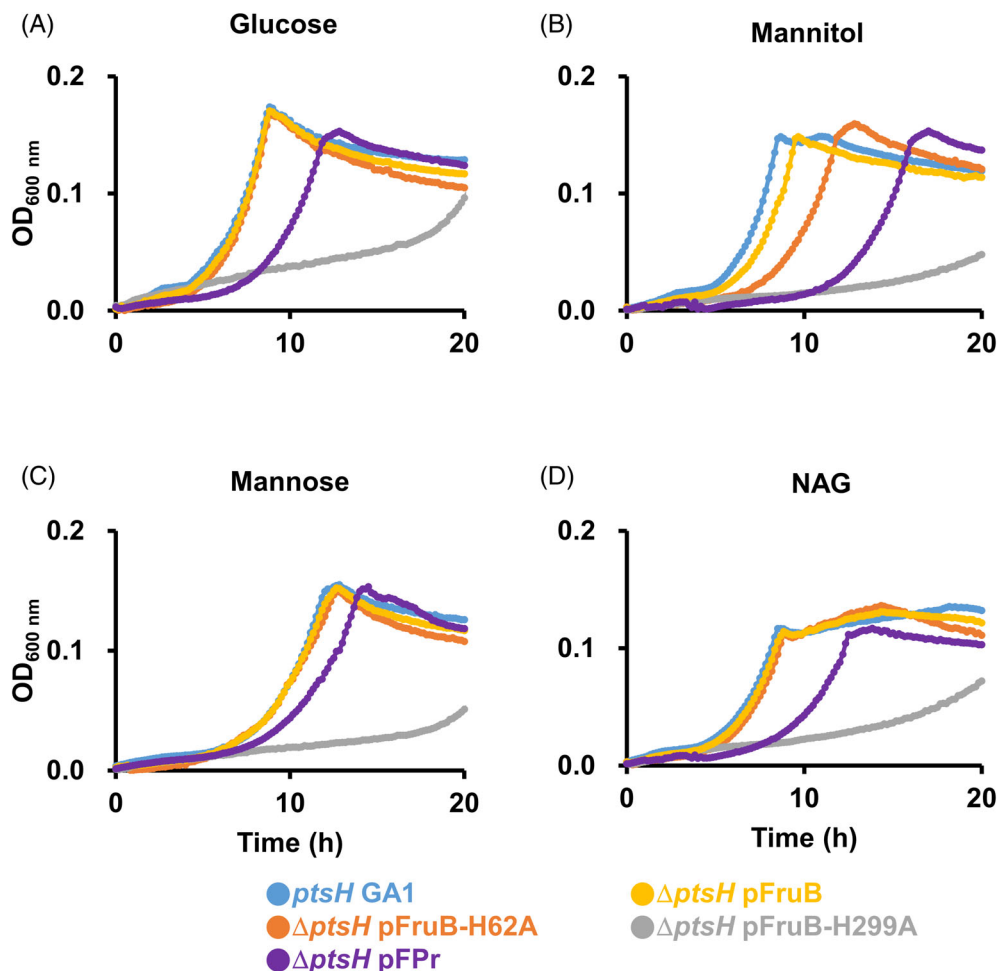


FIGURE 5 The FPr domain of FruB can replace the phosphotransferase activity of HPr in PTS sugar transport. The *ptsH* deletion mutant of the *E. coli* K12 strain MG1655 harbouring a pBR322-derived expression vector for a phosphorylation site mutant of FruB (pFruB-H62A or pFruB-H299A) or the wild-type FPr domain (pFPr) was incubated in M9 medium supplemented with 0.04% glucose (A), mannitol (B), mannose (C), or NAG (D), and its growth was compared to that of *ptsH* GA1 harbouring the control vector pBR322 and the *ptsH* deletion mutant carrying an expression vector for wild-type FruB (pFruB) in a 96-well plate by recording the absorbance at 600 nm using a multimode microplate reader (TECAN). Data shown are the averages of three measurements.

the wild-type strain, *ptsH* GA1 and the *ptsH cra* double deletion mutant had significantly higher intracellular cAMP levels when incubated in an M9 medium supplemented with the non-PTS sugar than in an M9 medium supplemented with glucose (Figure S8). It is noteworthy, however, that only PTS sugars, not the non-PTS sugars, can exert a selective pressure on the *ptsH* mutant (Figures 1, 2, and S2).

FruB catalyses the phosphotransferase reaction between EI and various EII_s in *ptsH* PA strains

Since FruB could catalyse the phosphotransferase reaction between EI and EIIA^{Glc}, we speculated that the efficient growth of the *ptsH* PA strains on other PTS sugars might depend on sugar-specific EII_s. To verify this, we generated mutants lacking *ptsG*, *mtlA*,

manXYZ, or *nagE* encoding EII_s specific for glucose, mannitol, mannose, or NAG, respectively, in *ptsH* GA1 and assessed their growth on relevant PTS sugars (Figure 7). While *ptsH* GA1 Δ *manXYZ* and *ptsH* GA1 Δ *mtlA* showed a complete loss of growth on mannose and mannitol, respectively, *ptsH* GA1 Δ *ptsG* and *ptsH* GA1 Δ *nagE* showed a moderate growth on glucose and NAG, respectively. Since ManXYZ is known to transport several hexoses, including glucose and NAG, as well as mannose (Plumbridge, 2009; Postma et al., 1993), we also constructed double deletion mutants of *ptsG manXYZ* and *nagE manXYZ* in *ptsH* GA1 and assessed their growth on glucose and NAG, respectively. As expected, both strains showed a complete loss of growth on relevant PTS sugars. Taken together, we concluded that FruB catalyses the phosphotransferase reaction between EI and various EII_s to efficiently transport PTS sugars instead of HPr in *ptsH* PA strains.

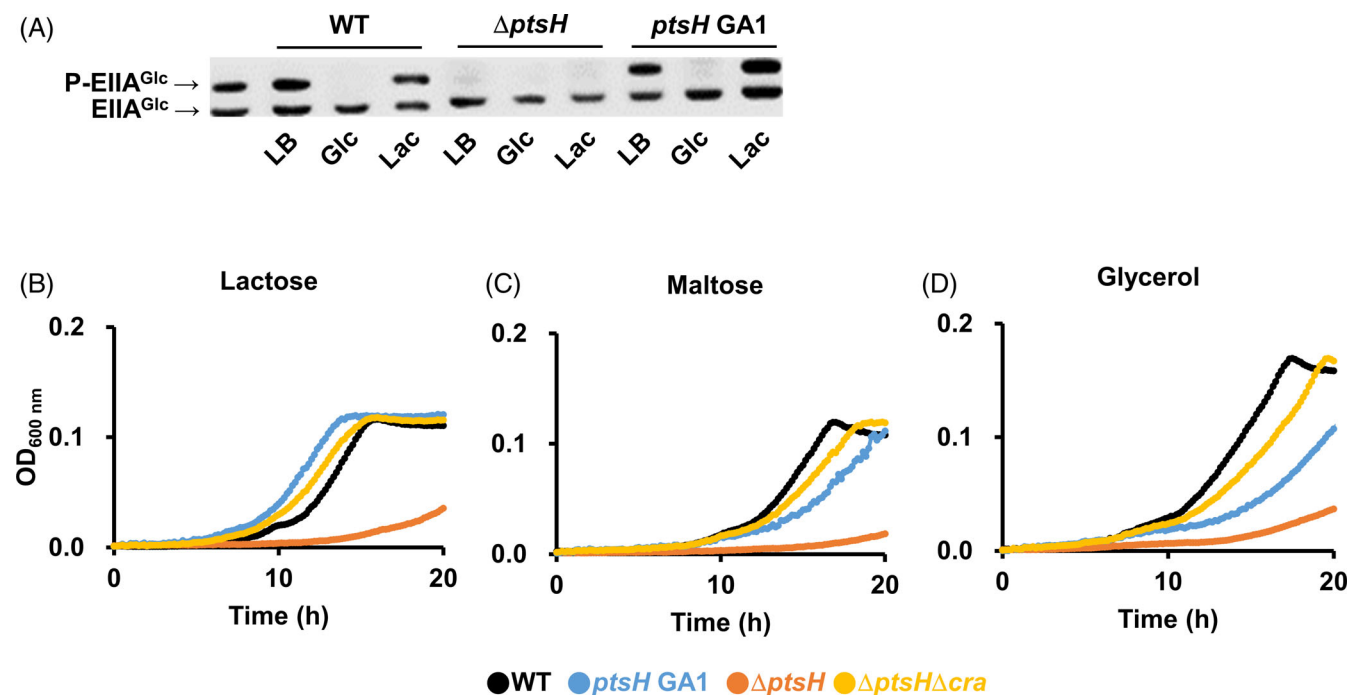


FIGURE 6 FruB can catalyse the phosphotransferase reaction between EI and EIIA^{Glc}. (A) The given *E. coli* K12 strains were incubated in an LB medium or M9 medium supplemented with 0.04% glucose (Glc) or lactose (Lac). The phosphorylation state of EIIA^{Glc} was determined when OD₆₀₀ reached 0.2 as described in the [Experimental Procedures](#). Purified EIIA^{Glc} (3 ng) was used as a positive control. (B–D) The *ptsH cra* double mutant and *ptsH* GA1 were incubated in M9 medium supplemented with 0.04% lactose (B), maltose (C), or glycerol (D), and their growth was compared to those of the wild type and *ptsH* mutant in a 96-well plate by recording the absorbance at 600 nm using a multimode microplate reader (TECAN). Data shown are the averages of three measurements.

Other paralogs of EI and HPr cannot replace EI and HPr in *E. coli*

The PTS of *Pseudomonas putida* encompasses only one carbohydrate (fructose)-related system and a nitrogen-related system (Pfluger-Grau & de Lorenzo, 2014). Unlike *E. coli* FruB, FruB in *P. putida* consists of three domains: EIIA, HPr and EI. A previous study found that both the EI and HPr domains of FruB can functionally replace PtsP (an EI paralog) and NPR (an HPr paralog) of the nitrogen PTS branch in *P. putida*, respectively (Pfluger & de Lorenzo, 2008). Within the *E. coli* genome, five EI and six HPr paralogs are encoded (Figure S7) (Tchieu et al., 2001). In these paralogs, the residues near the active site histidine residue responsible for the phosphotransferase activity tend to be more conserved than other parts. Among these paralogs, FryA, PtsA and DhaM contain both the EI and HPr domains; the amino acid residues of FryA and PtsA near each active site histidine residue of both EI and HPr domains appear to be more conserved than those in other paralogs (Figure S7A,B). Since the increased level of FruB could replace the phosphotransferase activity of HPr, we assumed that overexpression of other paralogs of EI and HPr might overcome the absence of EI and HPr in PTS sugar transport, respectively. To verify this assumption, we

constructed pBR322-derived expression vectors for the paralogs of EI and HPr under the control of the *cat* promoter, and determined whether the *ptsI* and *ptsH* mutants harbouring these vectors could recover their growth on PTS sugars (Figure S9). Interestingly, none of the EI paralogs could restore the growth of the *ptsI* mutant on PTS sugars and no other HPr paralogs than FruB could complement the growth defect of the *ptsH* mutant. These data might reflect why the *ptsI* mutant does not exhibit leaky growth phenotypes, while the *ptsH* mutant does, on various sugars (Baba et al., 2006; Simoni et al., 1976) and the *ptsI* mutant takes a much longer time to adapt to a medium with a PTS sugar than does the *ptsH* mutant.

The EI domains of FryA and PtsA have slightly higher identities with EI (39.1% and 37.7%, respectively) than that between the FPr domain of FruB and HPr (36.5%) (Figure S7C). Next, we determined the reason behind FruB, among the paralogs of general PTS components, being the only one that could replace the phosphotransferase activity of HPr in PTS sugar transport. Modern prediction tools of protein structure, such as AlphaFold and RoseTTAFold, are based on the co-evolutionary analysis (AlQuraishi, 2019). The phylogenetic tree analysis of six HPr paralogs revealed a closer evolutionary relationship of HPr with FruB than with other HPr paralogs. Although the phylogenetic tree

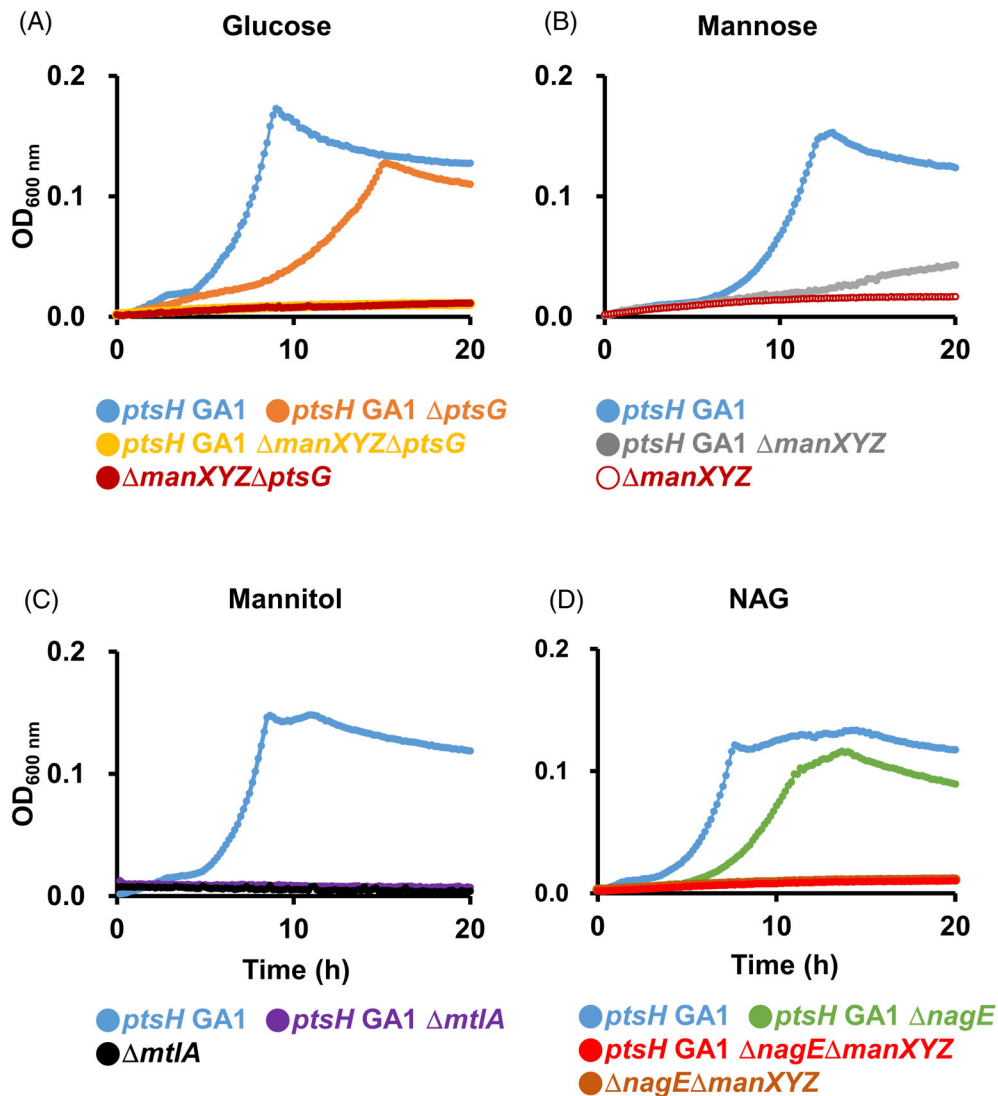


FIGURE 7 FruB catalyses the phosphotransferase reaction between EI and various EIs in *ptsH* PA strains. The chromosomal deletion mutants of *ptsG*, *mtlA*, *manXYZ*, and *nagE* genes encoding sugar-specific EIs in *ptsH* GA1 of the *E. coli* MG1655 were incubated in an M9 medium supplemented with 0.04% glucose (A), mannose (B), mannitol (C), or NAG (D), and their growth was compared to that of *ptsH* GA1 in a 96-well plate by recording the absorbance at 600 nm using a multimode microplate reader (TECAN). Data shown are the averages of three measurements.

analysis of six EI paralogs showed that PtsP has a closer evolutionary relationship with EI than does any other EI paralogs, the EI and PtsP pair has a much longer evolutionary distance than that of the HPr and FruB pair (Figure S7D). Therefore, this evolutionary history may explain why FruB can replace the phosphotransferase activity of HPr.

DISCUSSION

Several studies have shown that spontaneous genetic changes can occur when bacteria are cultured for long periods of time in a stressful environment (Poursat et al., 2019; Shewaramani et al., 2017; Taylor, 1963; Warsi et al., 2018). For example, in a previous study, it

took at least 70 h to isolate glucose-adapted colonies from the *E. coli* PB11 strain, which lacks both general PTS components (Aguilar et al., 2012). In this study, we evaluated the ability of an *E. coli ptsH* mutant to undergo adaptive genetic changes to utilize various sugars. The *ptsH* mutant underwent adaptive genetic changes in less than one generation time when incubated with any PTS sugars, except for fructose, as the sole carbon source. Only PTS sugars could induce immediate Cra mutations in the *ptsH* mutant, resulting in its leaky growth phenotypes on a PTS sugar (Figures 1, 2, and S2 and Table S1). Since other studies have shown that bacteria could undergo different genetic changes even under the same stressful environment (Poursat et al., 2019; Shewaramani et al., 2017; Taylor, 1963), we speculated that each of

ptsH PA strains would carry a different type of genetic mutations. However, all *ptsH* PA strains we isolated had loss-of-function mutations in *cra* (Table S1). We found that the mutations in *cra* resulted in constitutive expression of the *fru* operon and thus the FPr domain in FruB could replace the phosphotransferase activity of HPr in PTS sugar transport (Figure 5). Thus, in the case of the *ptsH* mutant, PTS sugar appears to act as strong selective pressure for genetic changes so that the resulting mutant can utilize various PTS sugars, such as glucose, mannitol, mannose, and NAG, as efficiently as the wild-type strain (Figures 4 and S4). However, although *ptsH* PA strains could utilize some non-PTS sugars as efficiently as the wild-type strain (Figure 6), none of these sugars could act as a selective pressure for genetic changes in the *ptsH* mutant (Figure 1). Therefore, it would be interesting to elucidate the molecular mechanism by which PTS sugars exert a strong selective pressure to induce Cra mutations in the *ptsH* mutant.

While HPr is highly conserved in both Gram-negative and Gram-positive bacteria (Postma et al., 1993; Reizer et al., 1992), FruB is conserved only in the families *Enterobacteriaceae*, *Pasteurellaceae*, and *Vibrionaceae* (Comas et al., 2008). We next questioned why species in these families have evolved to carry both HPr and FPr, which can replace the phosphotransferase activity of HPr (Geerse et al., 1986; Monedero et al., 1998). A previous study suggested that the *fru* operon was present in the last common ancestor of these families and FruB was modified to its current structure before the differentiation of these lineages (Comas et al., 2008). In several bacterial species, HPr plays an important role in regulating transcriptional regulators and metabolic genes for sugar utilization. For example, in *E. coli*, dephosphorylated HPr binds Rsd and antagonizes its stimulatory effect on SpoT (p) ppGpp hydrolase and anti- σ^{70} activities (Lee et al., 2018; Park et al., 2013). In addition, dephosphorylated HPr, accumulated during glucose transport, interacts with the mannitol operon regulator, MtlR, and enhances its repressor activity (Choe et al., 2017). Therefore, HPr and FPr might have diverged for more efficient regulation of metabolism and to meet varying metabolic needs in some bacterial species.

AUTHOR CONTRIBUTIONS

Huitae Min generated data. Huitae Min and Yeong-Jae Seok designed the study, analysed the results, and drafted the manuscript.

ACKNOWLEDGEMENTS

The authors thank Hye-Young Lee (Seoul National University) for the helpful discussions. This work was supported by National Research Foundation Grants NRF-2018R1A5A1025077 and NRF-2019R1A2C2004143 funded by the Ministry of Science, South Korea.

CONFLICT OF INTEREST

The authors have no conflicts of interest to declare.

DATA AVAILABILITY STATEMENT

The data that support the findings of this study are available from the corresponding author, Yeong-Jae Seok, upon reasonable request.

REFERENCES

- Aguilar, C., Escalante, A., Flores, N., de Anda, R., Riveros-McKay, F., Gosset, G. et al. (2012) Genetic changes during a laboratory adaptive evolution process that allowed fast growth in glucose to an *Escherichia coli* strain lacking the major glucose transport system. *BMC Genomics*, 13, 385.
- AlQuraishi, M. (2019) AlphaFold at CASP13. *Bioinformatics*, 35, 4862–4865.
- Baba, T., Ara, T., Hasegawa, M., Takai, Y., Okumura, Y., Baba, M. et al. (2006) Construction of *Escherichia coli* K-12 in-frame, single-gene knockout mutants: the Keio collection. *Molecular Systems Biology*, 2, 2006.008.
- Bluschke, B., Volkmer-Engert, R. & Schneider, E. (2006) Topography of the surface of the signal-transducing protein EIIA(Glc) that interacts with the MalK subunits of the maltose ATP-binding cassette transporter (MalFGK2) of *Salmonella typhimurium*. *The Journal of Biological Chemistry*, 281, 12833–12840.
- Choe, M., Park, Y.H., Lee, C.R., Kim, Y.R. & Seok, Y.J. (2017) The general PTS component HPr determines the preference for glucose over mannitol. *Scientific Reports*, 7, 43431.
- Comas, I., Gonzalez-Candelas, F. & Zuniga, M. (2008) Unraveling the evolutionary history of the phosphoryl-transfer chain of the phosphoenolpyruvate:phosphotransferase system through phylogenetic analyses and genome context. *BMC Evolutionary Biology*, 8, 147.
- Datsenko, K.A., & Wanner, B.L. (2000). One-step inactivation of chromosomal genes in *Escherichia coli* K-12 using PCR products. *Proceedings of the National Academy of Sciences*, 97, 6640–6645.
- Deutscher, J., Ake, F.M., Derkaoui, M., Zebre, A.C., Cao, T.N., Bouraoui, H. et al. (2014) The bacterial phosphoenolpyruvate: carbohydrate phosphotransferase system: regulation by protein phosphorylation and phosphorylation-dependent protein-protein interactions. *Microbiology and Molecular Biology Reviews*, 78, 231–256.
- Deutscher, J., Francke, C. & Postma, P.W. (2006) How phosphotransferase system-related protein phosphorylation regulates carbohydrate metabolism in bacteria. *Microbiology and Molecular Biology Reviews*, 70, 939–1031.
- Geerse, R.H., Ruig, C.R., Schuitema, A.R. & Postma, P.W. (1986) Relationship between pseudo-HPr and the PEP: fructose phosphotransferase system in *Salmonella typhimurium* and *Escherichia coli*. *Molecular & General Genetics*, 203, 435–444.
- Gorke, B. & Stulke, J. (2008) Carbon catabolite repression in bacteria: many ways to make the most out of nutrients. *Nature Reviews. Microbiology*, 6, 613–624.
- Hernández-Montalvo, V., Martínez, A., Hernández-Chavez, G., Bolívar, F., Valle, F., & Gosset, G. (2003). Expression of *galP* and *glk* in a *Escherichia coli* PTS mutant restores glucose transport and increases glycolytic flux to fermentation products. *Biotechnology and Bioengineering*, 83, 687–694.
- Hogema, B.M., Arents, J.C., Bader, R., Eijkemans, K., Yoshida, H., Takahashi, H. et al. (1998) Inducer exclusion in *Escherichia coli* by non-PTS substrates: the role of the PEP to pyruvate ratio in determining the phosphorylation state of enzyme IIAGlc. *Molecular Microbiology*, 30, 487–498.
- Kochanowski, K., Volkmer, B., Gerosa, L., Haverkorn van Rijsewijk, B.R., Schmidt, A. & Heinemann, M. (2013)

- Functioning of a metabolic flux sensor in *Escherichia coli*. *Proceedings of the National Academy of Sciences of the United States of America*, 110, 1130–1135.
- Lee, J.W., Park, Y.H. & Seok, Y.J. (2018) Rsd balances (p)ppGpp level by stimulating the hydrolase activity of SpoT during carbon source downshift in *Escherichia coli*. *Proceedings of the National Academy of Sciences of the United States of America*, 115, E6845–E6854.
- Lee, C.-R., Park, Y.-H., Min, H., Kim, Y.-R., & Seok, Y.-J. (2019). Determination of protein phosphorylation by polyacrylamide gel electrophoresis. *Journal of Microbiology*, 57, 93–100.
- Monedero, V., Postma, P.W. & Perez-Martinez, G. (1998) Suppression of the ptsH mutation in *Escherichia coli* and *Salmonella typhimurium* by a DNA fragment from lactobacillus casei. *Journal of Bacteriology*, 180, 5247–5250.
- Negre, D., Bonod-Bidaud, C., Geourjon, C., Deleage, G., Cozzone, A. J. & Cortay, J.C. (1996) Definition of a consensus DNA-binding site for the *Escherichia coli* pleiotropic regulatory protein, FruR. *Molecular Microbiology*, 21, 257–266.
- Park, Y.H., Lee, B.R., Seok, Y.J. & Peterkofsky, A. (2006) In vitro reconstitution of catabolite repression in *Escherichia coli*. *The Journal of Biological Chemistry*, 281, 6448–6454.
- Park, Y.H., Lee, C.R., Choe, M. & Seok, Y.J. (2013) HPr antagonizes the anti-sigma70 activity of Rsd in *Escherichia coli*. *Proceedings of the National Academy of Sciences of the United States of America*, 110, 21142–21147.
- Penin, F., Geourjon, C., Montserret, R., Bockmann, A., Lesage, A., Yang, Y.S. et al. (1997) Three-dimensional structure of the DNA-binding domain of the fructose repressor from *Escherichia coli* by 1H and 15 N NMR. *Journal of Molecular Biology*, 270, 496–510.
- Pfluger, K. & de Lorenzo, V. (2008) Evidence of in vivo cross talk between the nitrogen-related and fructose-related branches of the carbohydrate phosphotransferase system of *Pseudomonas putida*. *Journal of Bacteriology*, 190, 3374–3380.
- Pfluger-Grau, K. & de Lorenzo, V. (2014) From the phosphoenolpyruvate phosphotransferase system to selfish metabolism: a story retraced in *Pseudomonas putida*. *FEMS Microbiology Letters*, 356, 144–153.
- Plumbridge, J. (2009) An alternative route for recycling of N-acetylglucosamine from peptidoglycan involves the N-acetylglucosamine phosphotransferase system in *Escherichia coli*. *Journal of Bacteriology*, 191, 5641–5647.
- Postma, P.W., Lengeler, J.W. & Jacobson, G.R. (1993) Phosphoenolpyruvate:carbohydrate phosphotransferase systems of bacteria. *Microbiological Reviews*, 57, 543–594.
- Poursat, B.A.J., van Spanning, R.J.M., de Voogt, P. & Parsons, J.R. (2019) Implications of microbial adaptation for the assessment of environmental persistence of chemicals. *Critical Reviews in Environmental Science and Technology*, 49, 2220–2255.
- Ramseier, T.M. (1996) Cra and the control of carbon flux via metabolic pathways. *Research in Microbiology*, 147, 489–493.
- Reizer, J., Reizer, A., Kornberg, H.L. & Saier, M.H. (1994) Sequence of the fruB gene of *Escherichia coli* encoding the diphosphoryl transfer protein (DTP) of the phosphoenolpyruvate: sugar phosphotransferase system. *FEMS Microbiology Letters*, 118, 159–162.
- Reizer, J., Sutrina, S.L., Wu, L.F., Deutscher, J., Reddy, P. & Saier, M.H., Jr. (1992) Functional interactions between proteins of the phosphoenolpyruvate:sugar phosphotransferase systems of *Bacillus subtilis* and *Escherichia coli*. *The Journal of Biological Chemistry*, 267, 9158–9169.
- Saier, M.H., Bromberg, F.G. & Roseman, S. (1973) Characterization of constitutive galactose permease mutants in *Salmonella typhimurium*. *Journal of Bacteriology*, 113, 512–514.
- Shewaramani, S., Finn, T.J., Leahy, S.C., Kassen, R., Rainey, P.B. & Moon, C.D. (2017) Anaerobically grown *Escherichia coli* has an enhanced mutation rate and distinct mutational spectra. *PLoS Genetics*, 13, e1006570.
- Shimada, T., Fujita, N., Maeda, M. & Ishihama, A. (2005) Systematic search for the Cra-binding promoters using genomic SELEX system. *Genes to Cells*, 10, 907–918.
- Simoni, R.D., Roseman, S. & Saier, M.H., Jr. (1976) Sugar transport. properties of mutant bacteria defective in proteins of the phosphoenolpyruvate: sugar phosphotransferase system. *The Journal of Biological Chemistry*, 251, 6584–6597.
- Taylor, A.L. (1963) Bacteriophage-induced mutation in *Escherichia coli*. *Proceedings of the National Academy of Sciences of the United States of America*, 50, 1043–1051.
- Takahashi, H., Inada, T., Postma, P., & Aiba, H. (1998). CRP down-regulates adenylate cyclase activity by reducing the level of phosphorylated IIAGLC, the glucose-specific phosphotransferase protein, in *Escherichia coli*. *Molecular and General Genetics MGG*, 259, 317–326.
- Tchieu, J.H., Norris, V., Edwards, J.S. & Saier, M.H. (2001) The complete phosphotransferase system in *Escherichia coli*. *Journal of Molecular Microbiology and Biotechnology*, 3, 329–346.
- Warsi, O.M., Andersson, D.I. & Dykhuizen, D.E. (2018) Different adaptive strategies in *E. coli* populations evolving under macro-nutrient limitation and metal ion limitation. *BMC Evolutionary Biology*, 18, 72.
- Yoon, C.-K., Kang, D., Kim, M.-K., & Seok, Y.-J. (2021). *Vibrio cholerae* FruR facilitates binding of RNA polymerase to the fru promoter in the presence of fructose 1-phosphate. *Nucleic Acids Research*, 49, 1397–1410.

SUPPORTING INFORMATION

Additional supporting information can be found online in the Supporting Information section at the end of this article.

How to cite this article: Min, H. & Seok, Y.-J. (2022) Phosphotransferase system sugars immediately induce mutations of Cra in an *Escherichia coli* ptsH mutant. *Environmental Microbiology*, 24(11), 5425–5436. Available from: <https://doi.org/10.1111/1462-2920.16244>